Front. Optoelectron. 2015, 8(3): 274–281
DOI 10.1007/s12200-015-0522-y

RESEARCH ARTICLE

Blue fluorophores comprised of tetraphenylethene and imidazole: aggregation-induced emission and electroluminescence

Jiayun XIANG[1], Han NIE[2], Yibin JIANG[3], Jian ZHOU[1], Hoi Sing KWOK[3], Zujin ZHAO (✉)[1,2], Ben Zhong TANG (✉)[2,4]

1 College of Material, Chemistry and Chemical Engineering, Hangzhou Normal University, Hangzhou 310036, China
2 Guangdong Innovative Research Team, State Key Laboratory of Luminescent Materials and Devices, South China University of Technology, Guangzhou 510640, China
3 Center for Display Research, The Hong Kong University of Science & Technology, Kowloon, Hong Kong, China
4 Department of Chemistry, Division of Biomedical Engineering, Division of Life Science, The Hong Kong University of Science & Technology, Kowloon, Hong Kong, China

Abstract By melting tetraphenylethene (TPE) and 1,2,4,5-tetraphenyl-1H-imidazole (TPI) units together through different linking positions, three new fluorophores are synthesized, and their optical, electronic and electroluminescence (EL) properties are fully studied. Owing to the presence of TPE unit(s), these fluorophores are weak emitters in solutions, but are induced to emit strongly in the aggregated state, presenting typical aggregation-induced emission characteristics. The experimental and computational results reveal that different connection patterns between TPE and TPI could impact the molecular conjugation greatly, leading to varied emission wavelength, fluorescence quantum yield and EL performance in organic light emitting diodes (OLEDs). The fluorophore built by attaching TPE unit to the 1-position of imidazole ring shows bluest fluorescence, and its EL device emits at deep blue region (445 nm; CIE = (0.16, 0.15)). And the device based on the fluorophore by linking TPE to the 2-position of imidazole ring shows EL at 467 nm (CIE = (0.17, 0.22)) with good efficiencies of 3.17 $cd \cdot A^{-1}$, and 1.77%.

Keywords aggregation-induced emission (AIE), tetraphenylethene (TPE), imidazole, blue fluorescence, organic light emitting diode (OLED)

Received March 28, 2015; accepted May 25, 2015

E-mail: mszjzhao@scut.edu.cn, tangbenz@ust.hk

1 Introduction

Recently, great efforts have been devoted to develop efficient solid-state emitters for their various potential applications in organic light emitting diodes (OLEDs) [1], organic lasers [2], fluorescent sensors [3], etc. Many conventional π-conjugated fluorophores, however, suffer from the notorious aggregation-caused quenching (ACQ) effect: they emit strongly in the dilute solutions but become faintly fluorescent in the condense phase due to the formation of detrimental species such as excimers [4], which has obstructed their high-technological applications because the fluorophoric molecules are commonly used as solid films or nanoparticles in the real-world applications. To solve this ACQ problem, various molecular engineering approaches and device fabrication techniques had been proposed, but these attempts often ended with only limited success and even led to some side effects in many cases [5,6].

In 2001, an abnormal phenomenon, termed as aggregation-induced emission (AIE), was reported by Tang's group [7], which had been proved to be an effective approach to solve the ACQ problem. The AIE fluorophores are almost non-luminescent in dilute solutions but exhibit efficient emissions in the aggregated state. A series of designed experiments and the theoretical calculations were performed, and restriction of intramolecular rotations (RIR) was rationalized to be the main working mechanism behind this novel photophysical phenomenon [8]. Among the typical AIE fluorophores, tetraphenylethene (TPE) and many of its derivatives enjoy the advantages of easy

synthesis and outstanding AIE characteristic. Plenty of TPE derivatives can fluoresce intensely in solid state, and have been extensively used to fabricate efficient non-doped OLEDs [9–11].

As a typical heterocyclic molecule, imidazole has several substitution positions (N1, C2, C4 and C5), and many of its derivatives have been used extensively in OLEDs with high electroluminescence (EL) efficiencies, and good CIE coordinates in EL spectra [12–14]. In this work, we designed and successfully synthesized three new fluorophores (**1**-**3**) (Scheme 1) by melting the 1, 2, 4, 5-tetraphenyl-1H-imidazole (TPI) group and TPE unit in different patterns. The photoluminescence (PL) and EL properties of these new fluorophores were investigated. The OLEDs using the fluorophores as light-emitting layers were fabricated, which showed varied EL emission color from bluish green to deep blue, with moderate efficiencies.

2 Experimental

2.1 Materials and instruments

Tetrahydrofuran (THF) was distilled from sodium benzophenone ketyl under dry nitrogen immediately prior to use. Compounds 4-(1,2,2-triphenylvinyl)benzaldehyde (**5**) [15] and 4-(1,2,2-triphenylvinyl)aniline (**7**) [16] were prepared according to literature methods. All other chemicals and reagents were purchased from J&K Scientific Ltd., and used as received without further purification. ^{1}H and ^{13}C nuclear magnetic resonance (NMR) spectra were measured on a Bruker AV 500 or 400 spectrometer in deuterated chloroform using tetramethylsilane (TMS; $\delta = 0$) as internal reference. UV-vis absorption spectra were measured on a Shimadzu UV-2600 spectrophotometer. PL spectra were recorded on a Horiba Fluoromax-4 spectrofluorometer. Cyclic voltammetry (CV) was performed at room temperature by using a standard three-electrode electrochemical cell. The working and reference electrodes are platinum and saturated calomel electrode (SCE), respectively, with 0.1 M[1)] tetrabutylammonium hexafluorophosphate in acetonitrile solution as the supporting electrolyte at a scan rate of 50 mV· s^{-1}. The ground-state molecular geometrics were fully optimized and the electronic structures were investigated in THF solvent at the B3LYP/6-31G(d,p) level using the Gaussian 09 program. The polarizable continuum model (PCM) was employed for taking the solvent effect into account.

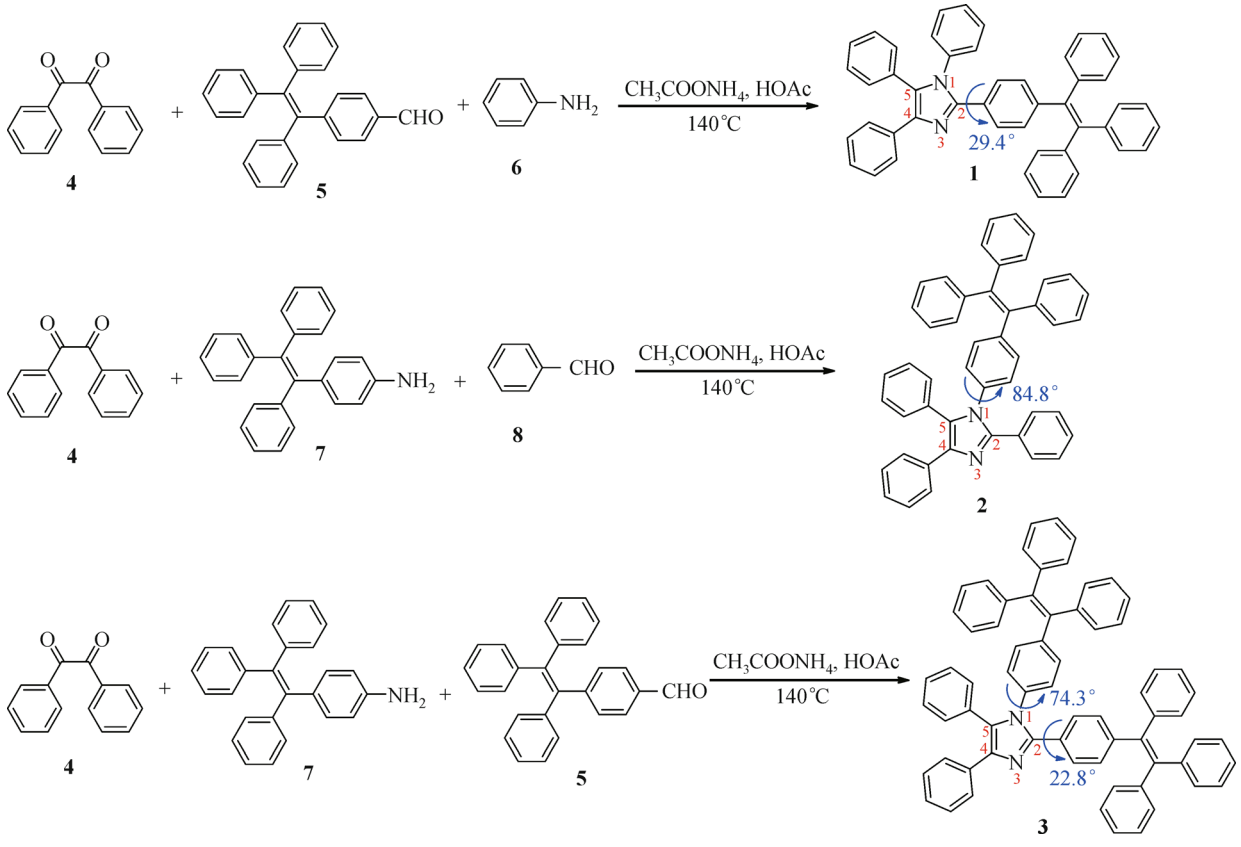

Scheme 1 Molecular structures and synthesis of the new fluorophores

1) 1M = 1 mol·L^{-1}

2.2 Synthesis

1,4,5-Triphenyl-2-(4-(1,2,2-triphenylvinyl)phenyl)-1H-imidazole (1): A mixture of 9,10-phenanthrenequinone (**4**) (0.42 g, 2 mmol), **5** (0.72 g, 2 mmol), aniline (**6**) (0.18 mL, 2 mmol) and ammonium acetate (1.28 g, 10 mmol) in glacial acetic acid (50 mL) was heated at 140°C under a nitrogen atmosphere for 12 h. After cooling to room temperature, the reaction mixture was poured into a methanol solution with stirring. The separated solid was filtered off, washed with methanol, and dried to give the raw product, which was further purified by silica-gel column chromatography using petroleum ether/dichloromethane as eluent. White solid was obtained in 93% yield. ^{1}H NMR (500 MHz, $CDCl_3$), δ (TMS, ppm[1)]): 7.61 (d, J = 7.5 Hz, 2H), 7.27–7.19 (m, 11H), 7.15–7.09 (m, 11H), 7.03–7.01 (m, 8H), 6.93 (d, J = 8.5 Hz, 2H). ^{13}C NMR (125 MHz, $CDCl_3$), δ (TMS, ppm): 146.81, 143.59, 143.54, 143.33, 141.46, 140.41, 137.00, 131.43, 131.35, 131.30, 131.14, 130.79, 128.99, 128.41, 128.36, 128.29, 128.16, 128.00, 127.69, 127.66, 127.46, 126.54, 126.51. HRMS ($C_{47}H_{34}N_2$): *m/z* 626.2609 (M^+, calcd 626.2722).

2,4,5-Triphenyl-1-(4-(1,2,2-triphenylvinyl)phenyl)-1H-imidazole (2): The procedure was analogous to that described for **1**. Pale brown solid, yield 85%. ^{1}H NMR (400 MHz, $CDCl_3$), δ (TMS, ppm): 7.60 (d, J = 6.8 Hz, 2H), 7.44 (d, J = 6.0 Hz, 2H), 7.27–7.21 (m, 9H), 7.09 (br, 11H), 6.99–6.91 (m, 8H), 6.77 (d, J = 8.0 Hz, 2H). ^{13}C NMR (100 MHz, $CDCl_3$), δ (TMS, ppm): 146.72, 144.19, 143.26, 143.15, 143.03, 141.91, 139.58, 135.02, 132.11, 131.31, 131.19, 131.14, 130.83, 129.02, 128.39, 128.26, 128.20, 128.04, 127.97, 127.83, 127.77, 127.48, 126.79, 126.74. HRMS ($C_{47}H_{34}N_2$): *m/z* 626.2708 (M^+, calcd 626.2722).

4,5-Diphenyl-1,2-bis(4-(1,2,2-triphenylvinyl)phenyl)-1H-imidazole (3): The procedure was analogous to that described for **1**. Green solid, yield 80%. ^{1}H NMR (500 MHz, $CDCl_3$), δ (TMS, ppm): 7.65 (br, 2H), 7.35–7.27 (m, 6H), 7.18–7.02 (m, 32H), 6.95 (d, J = 7.0 Hz, 6H), 6.73 (d, J = 8.0 Hz, 2H). ^{13}C NMR (125 MHz, $CDCl_3$), δ (TMS, ppm): 131.42, 131.38, 131.29, 131.18, 131.13, 127.83, 127.71, 126.73. HRMS ($C_{67}H_{48}N_2$): *m/z* 880.3798 (M^+, calcd 880.3817).

2.3 Device fabrication

The devices were fabricated on 80 nm Indium Tin Oxide (ITO)-coated glass with a sheet resistance of 25Ω/□. Prior to loading into the pretreatment chamber, the ITO-coated glass was soaked in ultrasonic detergent for 30 min, followed by spraying with de-ionized water for 10 min, soaking in ultrasonic de-ionized water for 30 min, and oven-baking for 1 h. The cleaned samples were treated by perfluoromethane plasma with a power of 100 W, gas flow of 50 sccm, and pressure of 0.2 Torr for 10 s in the pretreatment chamber. The samples were transferred to the organic chamber with a base pressure of 7×10^{-7} Torr for the deposition of NPB, emitter, and TPBi, which served as hole-transport, light-emitting, and electron-transport layers, respectively. The samples were then transferred to the metal chamber for cathode deposition which composed of lithium fluoride (LiF) capped with aluminum (Al). The light-emitting area was 4 mm^2. The current density-voltage characteristics of the devices were measured by a HP4145B semiconductor parameter analyzer. The forward direction photons emitted from the devices were detected by a calibrated UDT PIN-25D silicon photodiode. The luminance and external quantum efficiencies of the devices were inferred from the photocurrent of the photodiode. The electroluminescence spectra were obtained by a PR650 spectrophotometer. All measurements were carried out under air at room temperature without device encapsulation.

3 Results and discussion

3.1 Optical property

Figure 1(a) shows the absorption spectra of these new fluorophores in THF solutions. **1** and **2** exhibit absorption maxima at 337 and 290 nm, respectively, indicating that **2** possesses shorter effective conjugation length compared to **1**. Although the maximum absorption peak of **3** is located at 307 nm, its absorption spectral profile presents a long and strong tail at the longer wavelength region, which makes **3** and **1** have the same optical bandgaps (E_{opt} = 3.20 eV, Table 1) estimated from the onset wavelength of their absorption spectra, indicative of the similar conjugation length of both molecules.

The emissions of these new fluorophores are very weak in solutions. Their PL spectra in dilute THF solutions (10^{-5} M) only exhibit noisy signals without discernible peaks. And the fluorescence quantum yields (Φ_F) of **1**, **2** and **3** are merely 0.1%, 1.3% and 1.0% (Table 1), respectively, manifesting that they are indeed weak emitters when molecularly dissolved in good solvent. However, they emit very strong fluorescence when fabricated into thin solid films. As shown in Fig. 1(b), the emission maxima of **1** and **3** in solid films are located at 490 and 482 nm, being red-shifted relative to that of **2** in solid film (469 nm) due to their better conjugations. The Φ_F values of **1**, **2** and **3** in solid films are increased to 72.8%, 37.0% and 50.7%, respectively, revealing that they are AIE-active and excellent solid-state light emitters. This makes them promising candidates for the fabrication of efficient OLED devices. Understandably, owing to the presence of TPE units, the intramolecular rotation is active in these

1) 1 ppm = 1×10^{-6}

fluorophores when they are molecularly dissolved in THF solutions, which effectively deactivates the excited state via a nonradiative relaxation channel. The intramolecular rotations, however, are restricted by steric constraint in solid films, and thus the nonradiative decay channel is blocked, rendering the molecules emissive in solid films.

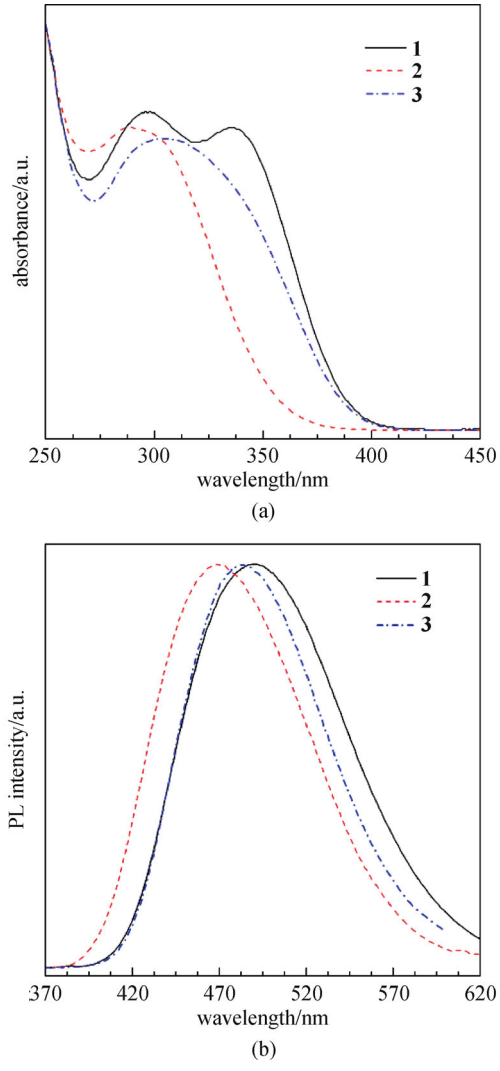

Fig. 1 (a) Absorption spectra in THF solutions (10^{-5} M) and (b) PL spectra in solid films of the new fluorophores

3.2 Electrochemical property

The electrochemical properties of these new fluorophores were investigated by CV. The voltammograms are presented in Fig. 2 and the obtained energy levels are summarized in Table 1. **1** and **3** exhibit oxidation onset potentials (E^{ox}_{onset}) at 1.11 and 1.13 V, respectively, both of which are lower than that of **2** (1.38 V). According to the following equation: HOMO = − (4.4 + E^{ox}_{onset}) eV, the HOMO energy levels are calculated to be −5.51, −5.78 and −5.53 eV for **1**, **2** and **3**, respectively. Their LUMO energy levels [LUMO = − (HOMO + E_{opt}) eV] could be determined from HOMO and E_{opt} values. As a result, these three fluorophores give similar LUMO energy levels: − 2.31 eV for **1**, − 2.30 eV for **2** and − 2.33 eV for **3.**

3.3 Theoretical calculation

To further study the photophysical properties of these new fluorophores, theoretical calculations were performed using the Gaussian 09 program. The molecular geometrics were fully optimized and electronic structures were investigated at the ground state (S_0) in THF solvent at the B3LYP/6-31G(d,p) level [17]. The PCM was employed for taking the solvent effect into account. As we all know, the HOMO and LUMO are two very important orbitals for determining the photophysical properties of the fluorophores. Hence, the electron density contours of HOMOs and LUMOs for these new fluorophores are illustrated in Fig. 3 and the corresponding orbital energy levels are summarized in Table 1. We found that the calculated values are basically consistent with the experimental data, which indicates this computational method is reasonable. The optimized molecular structures reveal that the torsion angles between TPE and TPI vary greatly in **1** (29.4°) and **2** (84.8°). As indicated in Scheme 1, when TPE is located at the 1-position of imidazole ring, the torsion angles are much larger than those when TPE are linked to the 2-positions of imidazole ring. This is indicative of a better conjugation of **1** and **3** than **2**. As shown in Fig. 3, the HOMOs of **1** and **3** are mainly located on the central imidazole core and 4,5-positioned phenyl rings and 2-positioned TPE unit, which endows them with similar HOMO energy levels. The HOMO of **2,** however, allows the electrons to be only delocalized over the central imidazole core and 2,4,5-positioned phenyl rings. Obviously, **1** and **3** have more extended conjugation than **2**, resulting in a much lower HOMO energy level of **2** than those of **1** and **3**. The LUMOs of the **1**, **2** and **3** are mainly localized on TPE unit(s). Based on above reasonable explanations, the much redder absorption and emission maxima of **1** and **3** relative to **2** become understandable. In comparison with TPE, TPI appears to be an electron-donating group. To confirm this, the energy levels of TPE and TPI are further calculated individually. According to the calculation results, the TPI unit has a higher HOMO energy level (−5.22 eV) than TPE (−5.33 eV), while TPE possesses a lower LUMO energy level (−1.22 eV) than TPI (−0.85 eV). Therefore, TPI and TPE units should serve as electron-donor and acceptor in these molecules, respectively.

3.4 Electroluminescence

The efficient emissions of **1**, **2** and **3** films encourage us to study their EL properties. Non-doped OLED devices with a configuration of ITO/NPB (60 nm)/EML (20 nm)/TPBi

Table 1 Optical properties and energy levels of the new fluorophores

	λ_{abs}[a)]/nm	λ_{em}[b)]/nm	Φ_F[c)]/%		(HOMO/LUMO)[d)] /eV	E_{opt}[e)]/eV
			soln	film		
1	337	490	0.1	72.8	−5.51 (−5.27)/−2.31 (−1.48)	3.20
2	290	469	1.3	37.0	−5.78 (−5.44)/−2.30 (−1.48)	3.48
3	307	482	1.0	50.7	−5.53 (−5.26)/−2.33 (−1.50)	3.20

Notes: a) In THF solution (10^{-5} M). b) Spin-coated film. c) Fluorescence quantum yield determined by a calibrated integrating sphere. d) Experimental data determined by cyclic voltammetry and calculated values given in parentheses. e) Optical bandgap energy determined from the onset of absorption spectra. HOMO, highest occupied molecular orbital; LUMO: lowest unoccupied molecular orbital

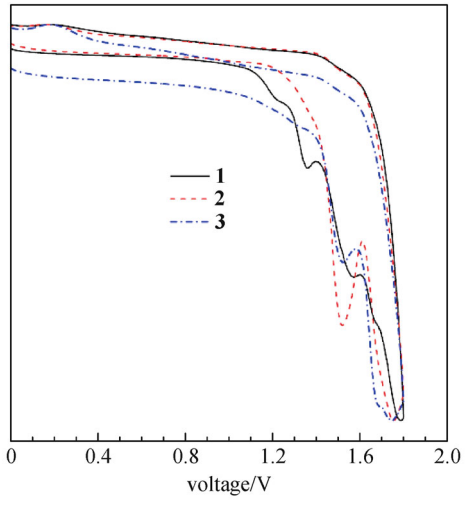

Fig. 2 CV curves of the new fluorophores in acetonitrile solution with 0.1 M tetrabutylammonium hexafluorophosphate as the supporting electrolyte at a scan rate of 50 $mV \cdot s^{-1}$

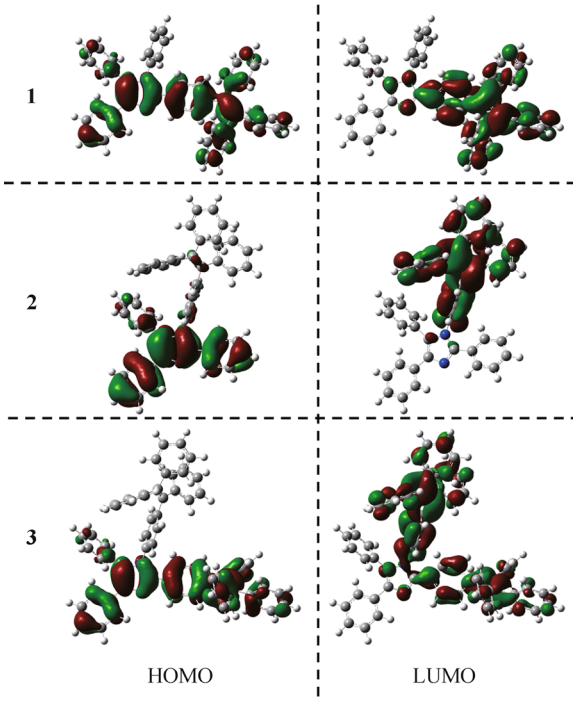

Fig. 3 Calculated molecular orbital amplitude plots of HOMOs and LUMOs for the new fluorphores

(40 nm)/LiF (1 nm)/Al (100 nm) were fabricated, where *N*, *N*′-di(1-naphthyl)-*N*,*N*′-diphenyl-benzidine (NPB) acted as a hole-transporting layer (HTL), 2,2′,2″-(1,3,5-benzinetriyl)-tris(1-phenyl-1H-benzimidazole) (TPBi) served as an electron-transporting layer (ETL) and the new fluorophores functioned as light-emitting layers (EML). Figure 4 shows the EL spectra, luminescence-voltage-current density characteristics and current efficiency versus current density curves of the OLEDs based on **1**, **2** and **3**. And the EL performance data are also summarized in Table 2. The EL devices based on **1**, **2** and **3** emit at 467, 445 and 495 nm with CIE chromaticity coordinates of (0.17, 0.22) (sky blue), (0.16, 0.15) (deep blue) and (0.21, 0.38) (bluish green), respectively. The EL peak of **3** is only slightly red-shifted from the PL peak (482 nm) of its solid film, confirming that the EL is indeed from the emitting layer. The EL spectra of **1** and **2**, however, are obviously blue-shifted from their PL spectra in solid films, implying that partial crystallization may happen in the emitting layer of the devices of **1** and **2**, because crystallization will cause blue-shifted emission in many TPE derivatives [18–20]. The devices of **1** and **3** show better performances than that of **2** due to the more efficient solid-state emission of **1** and **3**. The device of **1** is turned on at a low voltage of 3.6 V and exhibits a maximum luminance (L_{max}) of 5560 $cd \cdot m^{-2}$, a maximum current efficiency ($\eta_{C,max}$) of 3.12 $cd \cdot A^{-1}$, a maximum power efficiency ($\eta_{P,max}$) of 2.72 $lm \cdot W^{-1}$ and a maximum external quantum efficiency ($\eta_{ext,max}$) of 1.77%. The device based on **3** shows a similar performance compared to that of **1**, with turn-on voltage (V_{on}), L_{max}, $\eta_{C,max}$, $\eta_{P,max}$ and $\eta_{ext,max}$ of 4.4 V, 5110 $cd \cdot m^{-2}$, 3.97 $cd \cdot A^{-1}$, 2.43 $lm \cdot W^{-1}$, 1.58%, respectively. Since the conjugation of **2** is disrupted, its OLED device emits at deep blue region and shows inferior EL data (3620 $cd \cdot m^{-2}$, 0.96 $cd \cdot A^{-1}$, 0.75 $lm \cdot W^{-1}$ and 0.72%). According to the above results, the EL emission is tuned from bluish green to deep blue, realizing the control of EL emission and efficiency through a very simple strategy of minor structural modification.

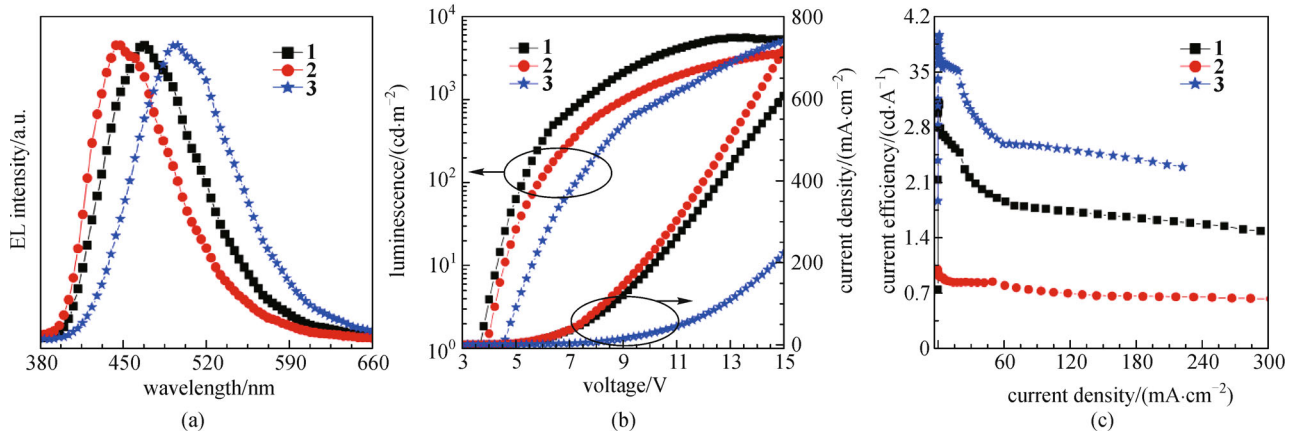

Fig. 4 (a) EL spectra; (b) current density-voltage-luminance characteristics; and (c) changes in current efficiency with the current density in multilayer EL devices of these new fluorophores [ITO/NPB (60 nm)/EML (20 nm)/TPBi (40 nm)/LiF (1 nm)/Al (100 nm)]

Table 2 EL performance of the new fluorophores[a)]

EML	λ_{EL}/nm	V_{on}/V	L_{max}/(cd·m^{-2})	η_C/(cd·A^{-1})	η_P/(lm·W^{-1})	EQE/%	CIE(x, y)
1	467	3.6	5560	3.12	2.72	1.77	(0.17, 0.22)
2	445	3.9	3620	0.96	0.75	0.72	(0.16, 0.15)
3	495	4.4	5110	3.97	2.43	1.58	(0.21, 0.38)

Notes: a) With a device configuration of ITO/NPB/EML/TPBi/LiF/Al. Abbreviation: EML = light-emitting layer, λ_{EL} = EL maximum, V_{on} = turn-on voltage at 1 cd·m^{-2}, L_{max} = maximum luminance, η_C = maximum current efficiency, η_P = maximum power efficiency, and EQE = maximum external quantum efficiency

4 Conclusions

In summary, three new fluorophores consisting of TPE and TPI units were prepared and their optical properties were investigated. They show very weak emissions when molecularly dissolved in dilute solutions, but they are induced to emit intensely in the solid films, demonstrating that they possess AIE characteristics. **1** and **3** exhibit longer effective π-conjugation lengths than **2**, which results in redder PL emissions and higher fluorescence quantum yields in the solid state. Non-doped EL devices of were fabricated using these fluorophores as emitters, and blue EL emissions with varied EL efficiencies were obtained. The impacts of a minor structural alternation on the PL and EL properties of the fluorophores have been demonstrated.

Acknowledgements We acknowledge the financial support from the National Natural Science Foundation of China (Grant Nos. 51273053, 21404029 and 21274034), the Guangdong Innovative Research Team Program of China (No. 201101C0105067115) and the National Basic Research Program of China (973 Program) (No. 2013CB834702).

References

1. Farinola G M, Ragni R. Electroluminescent materials for white organic light emitting diodes. Chemical Society Reviews, 2011, 40 (7): 3467–3482
2. Samuel I D W, Turnbull G A. Organic semiconductor lasers. Chemical Reviews, 2007, 107(4): 1272–1295
3. Basabe-Desmonts L, Reinhoudt D N, Crego-Calama M. Design of fluorescent materials for chemical sensing. Chemical Society Reviews, 2007, 36(6): 993–1017
4. Valeur B. Molecular Fluorescence: Principles and Applications. London: Wiley, 2001, 74–84
5. Grimsdale A C, Chan K L, Martin R E, Jokisz P G, Holmes A B. Synthesis of light-emitting conjugated polymers for applications in electroluminescent devices. Chemical Reviews, 2009, 109(3): 897–1091
6. Gaylord B S, Wang S, Heeger A J, Bazan G C. Water-soluble conjugated oligomers: effect of chain length and aggregation on photoluminescence-quenching efficiencies. Journal of the American Chemistry Society, 2001, 123(26): 6417–6418
7. Luo J, Xie Z, Lam J W Y, Cheng L, Chen H, Qiu C, Kwok H S, Zhan X, Liu Y, Zhu D, Tang B Z. Aggregation-induced emission of 1-methyl-1,2,3,4,5-pentaphenylsilole. Chemical Communications, 2001, 18(18): 1740–1741
8. Mei J, Hong Y, Lam J W Y, Qin A, Tang Y, Tang B Z. Aggregation-induced emission: the whole is more brilliant than the parts. Advanced Materials, 2014, 26(31): 5429–5479
9. Zhao Z, Lu P, Lam J W Y, Wang Z, Chan C Y K, Sung H H Y, Williams I D, Ma Y, Tang B Z. Molecular anchors in the solid state: restriction of intramolecular rotation boosts emission efficiency of fluorophore aggregates to unity. Chemical Science (Cambridge), 2011, 2(4): 672–675
10. Chen L, Jiang Y, Nie H, Hu R, Kwok H S, Huang F, Qin A, Zhao Z, Tang B Z. Rational design of aggregation-induced emission luminogen with weak electron donor-acceptor interaction to achieve highly efficient undoped bilayer OLEDs. ACS Applied Materials &

Interfaces, 2014, 6(19): 17215–17225
11. Liu Y, Chen S, Lam J W Y, Lu P, Kwok R T K, Mahtab F, Kwok H S, Tang B Z.Tuning the electronic nature of aggregation-induced emission fluorophores with enhanced hole-transporting property. Chemistry of Materials, 2011, 23(10): 2536–2544
12. Chou H H, Chen Y H, Hsu H P, Chang W H, Chen Y H, Cheng C H. Synthesis of diimidazolylstilbenes as *n*-type blue fluorophores: alternative dopant materials for highly efficient electroluminescent devices. Advanced Materials, 2012, 24(43): 5867–5871
13. Nagarajan N, Prakash A, Velmurugan G, Shakti N, Katiyar M, Venuvanalingam P, Renganathan R. Synthesis, characterisation and electroluminescence behaviourof π-conjugated imidazole-isoquinoline derivatives. Dyes and Pigments, 2014, 102: 180–188
14. Li W, Yao L, Liu H, Wang Z, Zhang S, Xiao R, Zhang H, Lu P, Yang B, Ma Y. Highly efficient deep-blue OLED with anextraordinarily narrow FHWM of 35 nm and a γ coordinate < 0.05 based on a fully twisting donor-acceptor molecule. Journal of Materials Chemistry C, 2014, 2(24): 4733–4736
15. Ma C, Xu B, Xie G, He J, Zhou X, Peng B, Jiang L, Xu B, Tian W, Chi Z, Liu S, Zhang Y, Xu J. An AIE-active luminophore with tunable and remarkable fluorescence switching based on the piezo and protonation-deprotonation control. Chemical Communications, 2014, 50(55): 7374–7377
16. Luo M, Zhou X, Chi Z, Liu S, Zhang Y, Xu J. Fluorescence-enhanced organogelators with mesomorphic and piezofluorochromic properties based on tetraphenylethylene and gallic acid derivatives. Dyes and Pigments, 2014, 101: 74–84
17. Frisch M J, Trucks G W, Schlegel H B, Scuseria G E, Robb M A, Cheeseman J R, Scalmani G, Barone V, Mennucci B, Petersson G A, Nakatsuji H, Caricato M, Li X, Hratchian H P, Izmaylov A F, Bloino J, Zheng G, Sonnenberg J L, Hada M, Ehara M, Toyota K, Fukuda R, Hasegawa J, Ishida M, Nakajima T, Honda Y, Kitao O, Nakai H, Vreven T, Montgomery J A Jr, Peralta J E, Ogliaro F, Bearpark M, Heyd J J, Brothers E, Kudin K N, Staroverov V N, Kobayashi R, Normand J, Raghavachari K, Rendell A, Burant J C, Iyengar S S, Tomasi J, Cossi M, Rega N, Millam N J, Klene M, Knox J E, Cross J B, Bakken V, Adamo C, Jaramillo J, Gomperts R, Stratmann R E, Yazyev O, Austin A J, Cammi R, Pomelli C, Ochterski J W, Martin R L, Morokuma K, Zakrzewski V G, Voth G A, Salvador P, Dannenberg J J, Dapprich S, Daniels A D, Farkas Ö, Foresman J B, Ortiz J V, Cioslowski J, Fox D J. Gaussian 09, Revision D.01. Gaussian Inc. Wallingford CT, 2009
18. Huang J, Sun N, Dong Y, Tang R, Lu P, Cai P, Li Q, Ma D, Qin J, Li Z. Similar or totally different: the control of conjugation degree through minor structural modifications, and deep-blue aggregation-induced emissionluminogens for non-doped OLEDs. Advanced Functional Materials, 2013, 23(18): 2329–2337
19. Zhao Z, Chen S, Shen X, Mahtab F, Yu Y, Lu P, Lam J W Y, Kwok H S, Tang B Z. Aggregation-induced emission, self-assembly, and electroluminescence of 4,4′-bis(1,2,2-triphenylvinyl)biphenyl. Chemical Communications, 2010, 46(5): 686–688
20. Zhao Z, Chen S, Lam J W Y, Lu P, Zhong Y, Wong K S, Kwok H S, Tang B Z. Creation of highly efficient solid emitter by decorating pyrene core with AIE-active tetraphenylethene peripheries. Chemical Communications, 2010, 46(13): 2221–2223

Jiayun Xiang received his B.S. degree in polymer materials from Hangzhou Normal University in 2012. He is now working toward his M.S. degree in the Zhao's group at Hangzhou Normal University. His research interest is mainly in the development of new aggregation-induced emission molecules and exploration of their optoelectronic device applications.

Han Nie received his B.S. degree in materials chemistry from Sichuan Normal University in 2012. He is now working toward his Ph.D. degree in the Tang's group at South China University of Technology. His research interest is mainly in the exploration of high-tech applications of aggregation-induced emission materials in optoelectronic devices.

Yibin Jiang received his B.S. degree in optical engineering from Zhejiang University in 2011. Now he is pursuing his Ph.D. degree in Department of Electronic & Computer Engineering at The Hong Kong University of Science and Technology. His research interests include organic light emitting diode technologies, quantum dot materials, and thin film transistor technologies.

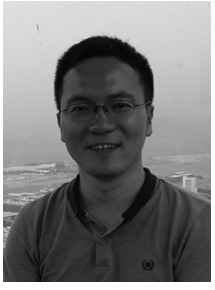

Jian Zhou received his Ph.D. degree in materials from Zhejiang University in 2009. He joined Hangzhou Normal University in 2010, where he is currently an associate professor. His current research focuses on the design and synthesis of functional conjugated polymers and exploration of their applications in sensors and optoelectronic devices.

Hoi Sing Kwok received his B.S. degree in electrical engineering from Northwestern University in 1973. He then studied with Professor Nicolaas Bloembergen (Nobel Laureate, 1981) at Harvard University, where he received his M.S. and Ph.D. degrees in applied physics in 1974 and 1978 respectively. From 1978 to 1980, he worked at the Lawrence Berkeley Laboratory with Professor Y. T. Lee (Nobel Laureate, 1986). From 1980 to 1992, he was in the Department of Electrical and Computer Engineering, State University of New York at Buffalo, where he was

a Professor since 1985. He joined The Hong Kong University of Science and Technology in 1992. He has chaired and was a member of program committees of many international conferences. He was awarded a US Presidential Young Investigator Award in 1984; the New York State/UUP Excellence Award in 1991. He is a Fellow of the Optical Society of America, a Fellow of IEEE and a Fellow of Society for Information Display.

Zujin Zhao received his B.S. degree in 2003 and Ph.D. degree in 2008 in chemistry from Zhejiang University. In 2008–2010, he conducted his postdoctoral work under supervision of Prof. Ben Zhong Tang at The Hong Kong University of Science and Technology. From 2010 to 2013, he worked in Hangzhou Normal University. Now, he is a full professor of State Key Laboratory of Luminescent Materials and Devices in South China University of Technology. His research is mainly focused on the development of efficient functional materials including organic small molecules and conjugated polymers and the exploration of their optoelectronic applications.

Ben Zhong Tang received his B.S. and Ph. D. degrees from South China University of Technology and Kyoto University in 1982 and 1988, respectively. He conducted his postdoctoral work at the University of Toronto and worked as a senior scientist in Neos Co., Ltd. in 1989 – 1994. Now he is a Chair Professor in the Department of Chemistry and Division of Biomedical Engineering, Stephen K. C. Cheong Professor of Science at The Hong Kong University of Science and Technology, and also honorary professor at South China University of Technology. He was elected to the Chinese Academy of Sciences in 2009. His research interest lies in the creation of new molecules with novel structures and unique properties with implications for high-tech applications. He is currently an Associate Editor of *Polymer Chemistry* and is on the editorial board of a dozen journals.